Optical Engineering 47(12), 125601 (December 2008)

Nano-roughness measurements with a modified Linnik microscope and the uses of full-field heterodyne interferometry

Yen-Liang Chen
Zhi-Cheng Jian
Hung-Chih Hsieh
Wang-Tsung Wu
Der-Chin Su, MEMBER SPIE
National Chiao Tung University
Department of Photonics and Institute of Electro-Optical Engineering
1001 Ta-Hsueh Road
Hsin-Chu 30050, Taiwan
E-mail: t7503@faculty.nctu.edu.tw

Abstract. A collimated heterodyne light enters a modified Linnik microscope, and the full-field interference signals are taken by a fast CMOS camera. The sampling intensities recorded at each pixel are fitted to derive a sinusoidal signal, and its phase can be obtained. Next, the 2-D phase unwrapping technique is applied to derive the 2-D phase distribution. Then, Ingelstam's formula is used to calculate the height distribution. Last, the height distribution is filtered with the Gaussian filter, the roughness topography and its average roughness can be obtained and its validity is demonstrated. [DOI: 10.1117/1.3050357]

Subject terms: roughness measurement; heterodyne interferometry; Linnik microscope; interference microscopy.

Paper 080524R received Jul. 3, 2008; revised manuscript received Nov. 4, 2008; accepted for publication Nov. 5, 2008; published online Dec. 22, 2008.

1 Introduction

The surface quality of optical and microelectronic components is very important for many manufacturing processes. The conventional stylus method is often used for surface roughness measurements. However, it has certain limitations. Among these, the stylus can potentially deform or damage the sample surface. In addition, the stylus travels slowly, so the measurement process is time consuming. To overcome these drawbacks, several nondestructive optical methods[1–7] have been proposed and have good measurement results. In this paper, an alternative method for measuring surface roughness with heterodyne interference microscopy is presented. The light beam coming from a heterodyne light source is collimated and enters a modified Linnik microscope, and the full-field interference signals are taken by a fast CMOS camera. Each pixel records a series of the sampling intensities of a sinusoidal signal. These sampling intensities are fitted[8] to derive the associated sinusoidal signal, and the phase of that pixel can be obtained. Then, the phase of any pixel can be obtained similarly. Next, the 2-D phase distribution can be determined with the 2-D phase unwrapping technique.[9] The height distribution can be derived with the data of the 2-D phase distribution and Ingelstam's formula.[10] Last, the data of the height distribution is filtered with the Gaussian filter defined by ISO 11562 (Ref. 11), and the roughness topography and its average roughness can be obtained. A roughness standard is tested to show the validity of this method. This method has some merits, such as simple optical configuration, high measurement accuracy, and rapid measurement.

2 Principle

Figure 1 shows a schematic diagram of this method. For convenience, the $+z$ axis is chosen to be along the light propagation direction, and the y axis is along the vertical direction. A light coming from a heterodyne light source[12] has a frequency difference f between the s- and the p-polarizations, and its Jones vector can be written as

$$E = \frac{1}{\sqrt{2}} \begin{bmatrix} \exp(i\pi f t) \\ \exp(-i\pi f t) \end{bmatrix}. \tag{1}$$

The light beam is expanded and collimated by a beam expander BE. It enters a modified Linnik microscope, which consists of a polarization beamsplitter PBS, a reference mirror M, two quarter-wave plates Q_1 and Q_2 with the fast axes at 45 deg with respect to the x axis, and two identical microscopic objectives MO_1 and MO_2. In addition, a test

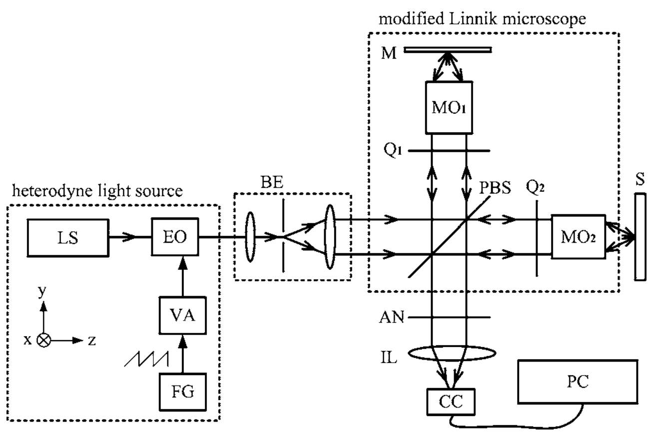

Fig. 1 Schematic diagram of this method. LS: laser light source; EO: electro-optic modulator; FG: function generator; VA: voltage amplifier; BE: beam expander; PBS: polarizing beamsplitter; Q: quarter-wave plate; MO: microscopic objective; M: mirror; S: sample; AN: analyzer; IL: imaging lens; CC: CMOS camera; and PC: personal computer.

0091-3286/2008/$25.00

sample S, an analyzer AN with the transmission axis at 45 deg with respect to the x axis, an imaging lens IL, and a CMOS camera CC are introduced into the optical configuration, which is also a modified Twyman-Greeen interferometer. In this interferometer, the paths of two collimated beams are (1) $\mathrm{PBS} \rightarrow \mathrm{Q}_1 \rightarrow \mathrm{MO}_1 \rightarrow \mathrm{M} \rightarrow \mathrm{MO}_1 \rightarrow \mathrm{Q}_1 \rightarrow \mathrm{PBS} \rightarrow \mathrm{AN} \rightarrow \mathrm{IL} \rightarrow \mathrm{CC}$ (the reference beam), and (2) $\mathrm{PBS} \rightarrow \mathrm{Q}_2 \rightarrow \mathrm{MO}_2 \rightarrow \mathrm{S} \rightarrow \mathrm{MO}_2 \rightarrow \mathrm{Q}_2 \rightarrow \mathrm{PBS} \rightarrow \mathrm{AN} \rightarrow \mathrm{IL} \rightarrow \mathrm{CC}$ (the test beam), respectively. Consequently, their amplitudes E_r and E_t can be expressed as

$$\begin{aligned} E_r &= AN(45^\circ) \cdot T_{\mathrm{PBS}} \cdot Q_1(-45^\circ) \cdot M \cdot Q_1(45^\circ) \cdot R_{\mathrm{PBS}} \cdot E \\ &= \frac{1}{2}\begin{pmatrix} 1 & 1 \\ 1 & 1 \end{pmatrix} \begin{pmatrix} 1 & 0 \\ 0 & 0 \end{pmatrix} \frac{1}{\sqrt{2}} \begin{pmatrix} 1 & i \\ i & 1 \end{pmatrix} \begin{pmatrix} -r_m & 0 \\ 0 & r_m \end{pmatrix} \\ &\quad \times \frac{1}{\sqrt{2}} \begin{pmatrix} 1 & -i \\ -i & 1 \end{pmatrix} \begin{pmatrix} 0 & 0 \\ 0 & 1 \end{pmatrix} \frac{1}{\sqrt{2}} \begin{bmatrix} \exp(i\pi f t) \\ \exp(-i\pi f t) \end{bmatrix} \\ &= \frac{i r_m}{4\sqrt{2}} \begin{pmatrix} 1 \\ 1 \end{pmatrix} \exp(-i\pi f t), \end{aligned} \tag{2}$$

and

$$\begin{aligned} E_t &= AN(45^\circ) \cdot R_{\mathrm{PBS}} \cdot Q_1(-45^\circ) \cdot S \cdot Q_1(45^\circ) \cdot T_{\mathrm{PBS}} \cdot E \\ &= \frac{1}{2}\begin{pmatrix} 1 & 1 \\ 1 & 1 \end{pmatrix} \begin{pmatrix} 0 & 0 \\ 0 & 1 \end{pmatrix} \frac{1}{\sqrt{2}} \begin{pmatrix} 1 & i \\ i & 1 \end{pmatrix} \\ &\quad \times \begin{bmatrix} -r_s \exp(i4\pi \cdot d/\lambda) & 0 \\ 0 & r_s \exp(i4\pi \cdot d/\lambda) \end{bmatrix} \\ &\quad \times \frac{1}{\sqrt{2}} \begin{pmatrix} 1 & -i \\ -i & 1 \end{pmatrix} \begin{pmatrix} 1 & 0 \\ 0 & 0 \end{pmatrix} \frac{1}{\sqrt{2}} \begin{bmatrix} \exp(i\pi f t) \\ \exp(-i\pi f t) \end{bmatrix} \\ &= -\frac{i r_s}{4\sqrt{2}} \begin{pmatrix} 1 \\ 1 \end{pmatrix} \exp\left(i\pi\left(ft + \frac{4d}{\lambda}\right)\right), \end{aligned} \tag{3}$$

where T_{PBS} and R_{PBS} are the transmission matrix and the reflection matrix of the PBS, r_m and r_s are the reflection coefficients of the M and the S, respectively; and $2d$ is the optical path difference between these two beams. Thus, the interference signals measured by the CC can be written as

$$\begin{aligned} I &= |E_r + E_t|^2 = I_0 + \gamma \cdot \cos(2\pi f t + \phi_0) = A \cdot \cos(2\pi f t) \\ &\quad + B \cdot \sin(2\pi f t) + C, \end{aligned} \tag{4}$$

where I_0 is the mean intensity; γ and ϕ_0 are the visibility and the phase, respectively, of the interference signal; and A, B, and C are real numbers. Moreover, ϕ_0 equals the phase difference between E_r and E_t. These values are

$$I_0 = \frac{1}{16}(r_m^2 + r_s^2), \tag{5}$$

$$\gamma = \frac{-r_m r_s}{8}, \tag{6}$$

and

$$\phi_0(x,y) = \frac{4\pi d}{\lambda} = \phi_1 + \phi_2 = 2n\pi + \phi_2 = 2n\pi + \tan^{-1}\left(\frac{-B}{A}\right), \tag{7}$$

where ϕ_1 is the phase of the reference point on the S. This equals $2n\pi$, where n is an integer, and can be omitted. ϕ_2 is the relative phase with respect to the reference point, and it depends on the height distribution $h(x,y)$ of the sample surface.

Next, the camera CC with the frame frequency f_c is used to record n frames at times $t_1, t_2, \ldots, t_n$. Each pixel records a series of interference intensities $I_1, I_2, \ldots, I_n$, which are the sampled intensities of a sinusoidal signal. Then, we have

$$\begin{pmatrix} I_1 \\ I_2 \\ \vdots \\ I_n \end{pmatrix} = M \cdot \begin{pmatrix} A \\ B \\ C \end{pmatrix}, \tag{8}$$

where

$$M = \begin{pmatrix} \cos 2\pi f t_1 & \sin 2\pi f t_1 & 1 \\ \cos 2\pi f t_2 & \sin 2\pi f t_2 & 1 \\ \vdots & \vdots & \vdots \\ \vdots & \vdots & \vdots \\ \cos 2\pi f t_n & \sin 2\pi f t_n & 1 \end{pmatrix}. \tag{9}$$

Equation (8) can be rewritten as

$$\begin{pmatrix} A \\ B \\ C \end{pmatrix} = (M^t M)^{-1} M^t \begin{pmatrix} I_1 \\ I_2 \\ \vdots \\ I_n \end{pmatrix}, \tag{10}$$

where M^t means the transpose matrix of M. Equation (10) can be solved by using the least-square fitting algorithm on IEEE Standards,[8] and the data of A and B can be obtained. These are substituted into Eq. (7), and the data of ϕ_2 can be derived. If these processes are applied to all other pixels, then the associated data $\phi_2(x,y)$ can be obtained similarly. Except the intrinsic electronic noises, the data $\phi_2(x,y)$ are easily influenced by the ambient motions because of the two-path optical configuration. To reduce the phase outliers and dropouts that often occur near groove edges, $\phi_2(x,y)$ are processed with the special algorithm for noisy phase-map processing.[13] In addition, the 2-D phase unwrapping technique[9] is applied to solve the phase ambiguity, and the full-field phase distribution $\phi(x,y)$ is obtained. In this method, the light beam is converged to incident on the S by using the MO_2 with numerical aperture NA, so the relation between $\phi(x,y)$ and the height distribution $h(x,y)$ of the S can be expressed as

$$h(x,y) = \frac{\lambda \cdot \phi(x,y)}{4\pi} \cdot k, \tag{11}$$

where k is a correction factor and can be expressed as

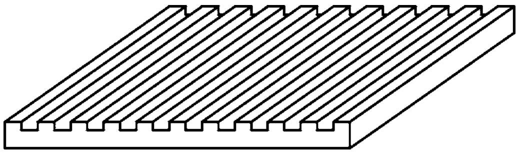

Fig. 2 The test sample, which is a roughness standard specimen with rectangular wave forms.

$$k = 1 + \frac{NA^2}{4}, \tag{12}$$

according to Ingelstam's formula.[10] If the derived data of $\phi(x,y)$ and the value of k obtained from Eq. (12) are substituted into Eq. (11), then $h(x,y)$ can be calculated.

Last, the Gaussian filter defined by ISO 11562 (Ref. 11) is then applied to subtract the waviness part of $h(x,y)$, and the roughness part $R(x,y)$ can be obtained. Based on the formula of 2-D roughness parameter defined by the ISO 25178-2 standard,[14] the average roughness value S_a is defined as

$$S_a = \frac{1}{UV}\sum_{k=0}^{U-1}\sum_{l=0}^{V-1}|R(x_k,y_l) - \mu|, \tag{13}$$

where $U \times V$ are the pixel numbers of one frame, and μ is the average of $R(x,y)$. Substituting the data of $R(x,y)$ and μ into Eq. (13), the data of S_a can be obtained.

3 Experiments and Results

To demonstrate the validity of this method, we tested a roughness standard specimen with rectangular wave forms, as shown in Fig. 2. The pitch of the rectangular wave forms is 20 μm. It was also measured with a commercial stylus instrument by the National Measurement Laboratory in Taiwan, and its average roughness value is 67 nm. An He-Ne laser with 632.8-nm wavelength, two 10× microscopic objectives with NA=0.25, and a CMOS camera (Basler/A504K) with 8-bit gray levels and 300×210 pixels were used in this test. Under the conditions f=20 Hz and f_c=300.3 frames/s, 300 frames were taken in 1 s. A least-squares sine fitting algorithm on the IEEE 1241 standard in a MATLAB program was utilized, and the data of $\phi_2(x,y)$ were obtained and are shown in Fig. 3. Then, the data of

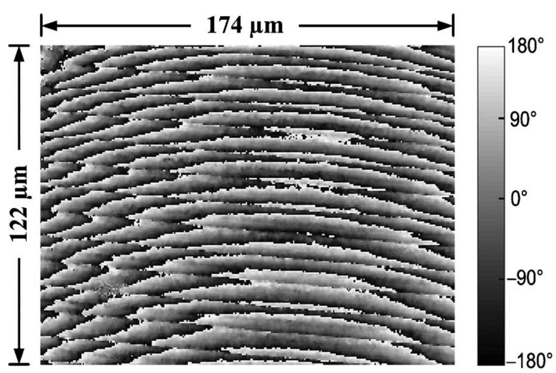

Fig. 3 The full-field phase distribution $\phi_2(x,y)$ in gray levels.

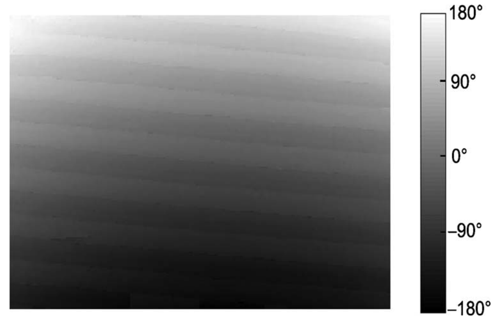

Fig. 4 The full-field phase distribution $\phi(x,y)$ in gray levels.

$\phi_2(x,y)$ were processed with the 2-D phase unwrapping technique, and the full-field phase distribution $\phi(x,y)$ were obtained and are shown in gray levels in Fig. 4. In addition, the data of $\phi(x,y)$ were substituted into Eq. (11) and the data of $h(x,y)$ were calculated. Last, the data of $h(x,y)$ were filtered by a bandpass Gaussian filter with the long cutoff wavelength λ_c=80 μm to reduce the waviness and the short cutoff wavelength λ_s=2.5 μm to eliminate the noise.[15,16] The full-field surface roughness topography $R(x,y)$ is shown in gray levels in Fig. 5; its average roughness can be calculated with Eq. (13) and obtained as S_a=65.7 nm.

4 Discussion

The profile along the white line in the inset in Fig. 5 was also measured by the contact stylus instrument. Their measured results are shown together in Fig. 6 for comparison: the solid curve is for this method, and the dotted curve is for the contact stylus instrument. From Fig. 6, it can be obtained that their cross-correlation function[17] is up to 91.5%. Because the total points with different measured results are less than 10%, both are acceptable.[18]

The phase distribution $\phi(x,y)$ is the relative data and is shifted as the optical configuration is rearranged. Despite the shift of $\phi(x,y)$, the measured results $R(x,y)$ have the same profile with a different value of μ. The data of S_a is

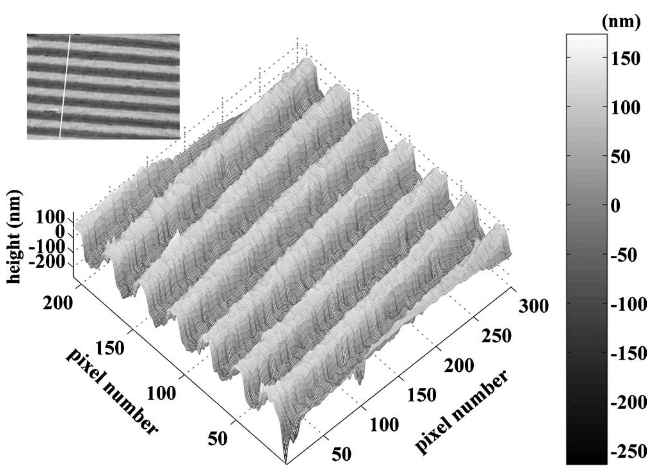

Fig. 5 The measured full-field roughness topography $R(x,y)$ in gray levels.

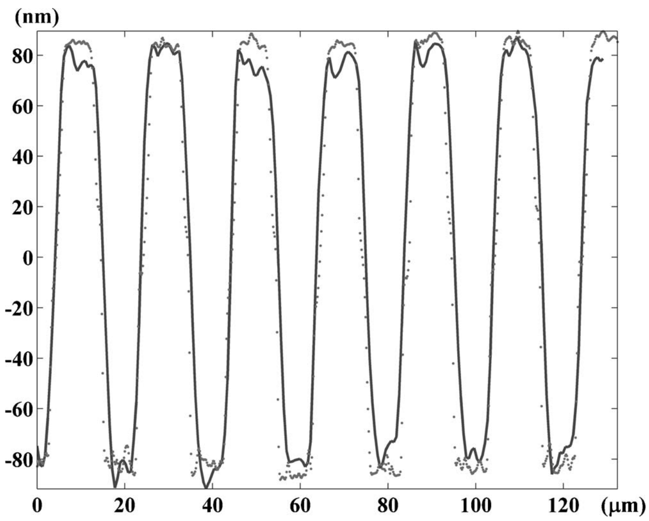

Fig. 6 Measured profiles along the white line in the inset in Fig. 5 with this method (solid curve) and the contact stylus instrument (dotted curve).

still unchanged. After filtering by the Gaussian filter, the surface waviness and the alignment error can be subtracted. The errors in this technique may be influenced by the following factors:

- **Sampling error**. This depends on the frequency of the heterodyne interference signal, the camera recording time, the frame period, the frame exposure time, and the number of gray levels. The condition f_c =300.3 frames/s is chosen based on the optimal condition proposed by Jian et al.[19] to decrease the measurement error, and the sampling error $\Delta\phi_s$ is about 0.036 deg.
- **Polarization-mixing error**. Owing to the extinction ratio effect of a polarizer, mixing of light polarization occurs. In our experiments, the extinction ratio of the polarizer (Japan Sigma Koki, Ltd.) is 1×10^{-5}. This can be estimated in advance to modify the measured results, and the polarization-mixing error can be decreased to $\Delta\phi_p$=0.03 deg with this modification.[20]

Consequently, the theoretical error of this method is

$$\Delta S_a = \Delta h = \frac{\lambda}{4\pi} k(\Delta\phi_s + \Delta\phi_p) = 0.06 \text{ nm}. \quad (14)$$

Hence, this method has better theoretical resolution than that of phase-shifting interferometry and white-light interferometry.[21]

5 Conclusion

In this paper, an alternative method for measuring full-field surface roughness has been proposed by introducing heterodyne interfermoetry into a modified Linnik microscope. The full-field interference signals are taken by a fast CMOS camera, and a series of the sample intensities of a sinusoidal signal are recorded at each pixel. The associated phase of each pixel can be derived with a least-squares sine fitting algorithm. The height distribution can be derived with the 2-D phase unwrapping technique and Ingelstam's formula. Last, the data of height distribution is filtered, and the roughness topography and its average roughness can be obtained. The method's validity has been demonstrated, and it has some merits, such as simple optical configuration, high measurement accuracy, and rapid measurement.

Acknowledgments

This study was supported in part by the National Science Council, Taiwan, under Contract No. NSC95-2221-E009-236-MY3.

References

1. J. M. Bennett, "Recent developments in surface roughness characterization," *Meas. Sci. Technol.* **3**, 1119–1127 (1992).
2. U. Persson, "Real time measurement of surface roughness on ground surface using speckle-contrast technique," *Opt. Lasers Eng.* **17**, 61–67 (1992).
3. R. Windecker and H. J. Tiziani, "Optical roughness measurements using extended white-light interferometry," *Opt. Eng.* **38**, 1081–1087 (1999).
4. S. H. Wang, C. Quan, C. J. Tay, and H. M. Shang, "Surface roughness measurement in the submicrometer range using laser scattering," *Opt. Eng.* **39**, 1597–1601 (2000).
5. C. Cheng, C. Liu, N. Zhang, T. Jia, R. Li, and Z. Xu, "Absolute measurement of roughness and lateral-correlation length of random surfaces by use of the simplified model of image-speckle contrast," *Appl. Opt.* **41**, 4148–4156 (2002).
6. A. Duparre, J. F. Borrull, S. Gliech, G. Notni, J. Steinert, and J. M. Bennett, "Surface characterization techniques for determining the root-mean-square roughness and power spectral densities of optical components," *Appl. Opt.* **41**, 154–171 (2002).
7. I. Yamaguchi, K. Kobayashi, and L. Yaroslavsky, "Measurement of surface roughness by speckle correlation," *Opt. Eng.* **43**, 2753–2761 (2004).
8. IEEE, "Standard for terminology and test methods for analog-to-digital converters," IEEE Std. 1241–2000, pp. 25–29 (2000).
9. D. C. Ghiglia and M. D. Pritt, "Two-dimensional phase unwrapping: theory, algorithms, and software," Wiley, New York (1998).
10. E. Ingelstam, "Problems related to the accurate interpretation of microinterferograms," *Interferometry, National Physical Laboratory Symposium* **11**, 41–163 (1960).
11. "Geometrical product specifications (GPS)—surface texture: profile method—metrological characteristics of phase correct filters," ISO 11562 (1996).
12. D. C. Su, M. H. Chiu, and C. D. Chen, "Simple two frequency laser," *Precis. Eng.* **18**, 161–163 (1996).
13. J. A. Quiroga and E. Bernabeu, "Phase-unwrapping algorithm for noisy phase-map processing," *Appl. Opt.* **33**, 6725–6731 (1994).
14. "Geometrical product specifications (GPS)—surface texture: areal—part 2: terms, definitions, and surface texture parameters," ISO/DIS 25178-2 (2008).
15. "Geometrical product specifications (GPS)—surface texture: profile method—rules and procedures for the assessment of surface texture," ISO 4288 (1996).
16. "Geometrical product specifications (GPS)—surface texture: profile method—nominal characteristics of contact (stylus) instruments," ISO 3274 (1996).
17. J. Song, T. Vorburger, T. Renegar, H. Rhee, A. Zheng, L. Ma, J. Libert, S. Ballou, B. Bachrach, and K. Bogart, "Correlation of topography measurements of NIST SRM 2460 standard bullets by four techniques," *Meas. Sci. Technol.* **17**, 500–503 (2006).
18. R. Krüger-Sehm and J. A. Luna Perez, "Proposal for a guideline to calibrate interference microscopes for use in roughness measurements," *Int. J. Mach. Tools Manuf.* **41**, 2123–2137 (2001).
19. Z. C. Jian, Y. L. Chen, H. C. Hsieh, P. J. Hsieh, and D. C. Su, "Optimal condition for full-field heterodyne interferometry," *Opt. Eng.* **46**, 115604 (2007).
20. M. H. Chiu, J. Y. Lee, and D. C. Su, "Complex refractive-index measurement based on Fresnel's equations and uses of heterodyne interferometry," *Appl. Opt.* **38**, 4047–4052 (1999).
21. H. G. Rhee, T. V. Vorburger, J. W. Lee, and J. Fu, "Discrepancies between roughness measurements obtained with phase-shifting and white-light interferometry," *Appl. Opt.* **44**, 5919–5927 (2005).

Yen-Liang Chen received his MS degree from the Department of Atomic Science, National Tsing Hua University, Taiwan, in 2000 and is now working toward his PhD degree in optical metrology at the Institute of Electro-Optical Engineering of National Chiao Tung University. His current research activities are in optical metrology.

Zhi-Cheng Jian received his MS degree from the Institute of Electro-Optical Engineering, National Taipei University of Technology, Taiwan, in 2002 and is now working toward a PhD degree in optical metrology at the Institute of Electro-Optical Engineering of National Chiao Tung University. His current research activities are in optical metrology.

Hung-Chih Hsieh received his MS degree from the Institute of Electro-Optical Engineering, National Chiao Tung University, Taiwan, in 2005 and is now working toward his PhD degree in optical metrology at the Institute of Electro-Optical Engineering of National Chiao Tung University. His current research activities are in optical metrology and nondestructive testing.

Wang-Tsung Wu received his BS degree in physics from the National Tsing Hua University, Taiwan, in 2006 and is now working toward his PhD degree in optical metrology at the Institute of Electro-Optical Engineering of National Chiao Tung University. His current research activities are in optical metrology and nondestructive testing.

Der-Chin Su received his BS degree in physics from the National Taiwan Normal University in 1975 and his MS and PhD degrees in information processing from the Tokyo Institute of Technology in 1983 and 1986, respectively. He joined the faculty of the National Chiao Tung University in 1986, where he is currently a professor with the Institute of Electro-Optical Engineering. His current research interests are in optical testing and holography.